

POSSIBILITIES OF DETERMINATION OF ALTERATION DEGREE OF ROCKS BY THERMOGRAVIMETRY

P. Rózsa^{1*}, S. Szakáll², Éva Balázs¹ and A. Bartha³

¹Department of Mineralogy and Geology, University of Debrecen, 4032 Debrecen, Egyetem tér 1, Hungary

²Department of Mineralogy and Petrology, University of Miskolc, 3515 Miskolc-Egyetemváros, Hungary

³Geological Institute of Hungary, 1143 Budapest, Stefánia út 14, Hungary

Rhyolite-rhyodacite tuff samples were analysed by X-ray powder diffraction, ICP-OES and thermogravimetric (TG) methods to determine mineral and major element composition as well as different types of bound water, respectively. Similarly to CIA values, some TG parameters ($H_2O[I]$ – water released up to ca. 200–220°C; $H_2O[III]$ – water loss above 500–550°C and $H_2O[I+III]$) show positive correlation to the amount of secondary minerals. Moreover, these parameters are in close positive correlation to CIA values. Our results suggest that TG determination of different types of bound water may serve as a useful tool for estimation and characterisation of alteration degree of rocks.

Keywords: alteration, bound water, thermogravimetry

Introduction

Weathering process means mineralogical, petrographical and geochemical alteration of rocks, therefore characterisation of weathered state is important for determining or predicting their physical and engineering properties. In general, weathering can be regarded as an acid-base reaction where an acid is neutralised by a solid base to produce secondary minerals and dissolved salts [1]. Essentially, weathering is a process of chemical reaction between rock (mineral) and water, as a result of which the water in the internal structure of minerals successively increases. As a consequence, a negative correlation was found between water content and different mechanical constituents [2]. Moreover, different types of bonding water in soils can be used for estimating geotechnical data [3, 4]. On the basis of the well-known experience that increasing total water content may reflect increasing alteration, the simple index of chemical weathering degree (CWD) described by the following equation was proposed:

$$CWD = \frac{100(W_w - W_f)}{(W_u - W_f)} [\%]$$

where W_w is the combined water in weathered rock (%), W_f is the combined water in fresh rock (%), W_u is the combined water in the ultimate weathering product (%) [5]. Some authors, however, regard the ‘ultimate weathering product’ to be very subjective to define, and they do not recommended CWD to use [6]. Although this argument can be accepted, it seems to be logic

that H_2O content could and should be considered an indicator of the degree of weathering. Thermal analysis makes possible to distinguish different types of bound waters in minerals [7], therefore it could be more suitable for characterisation of weathering process than determination of total water content. Molecular water content and the amount of hydroxyl of clay minerals can be easily measured by thermoanalysis, and these parameters indicate the weathering degree [8–10]. In this paper comparison of analyses of rhyolite-rhyodacite tuff samples are presented. The mineralogical and major element composition of the samples was determined by X-ray diffraction and ICP-OES techniques, respectively; quantitative measurement of different types of bound water ($H_2O[I]$ – molecular water in minerals released up to ca. 200–220°C; $H_2O[II]$ – water loss between ca. 200–220 and 500–550°C; $H_2O[III]$ – water loss above 500–550°C) was carried out by thermogravimetric (TG) method.

Experimental

Ten samples were collected in Eger town (NE Hungary) and its near environment. Topographical positions of the sampling point were recorded by GPS, and then marked in a geological sketch map. The sampled formations are Miocene in age. Two samples belong to the Gyulakeszi Rhyolite Tuff Formation (Ottangian), three of them represent the Felnémet Rhyolite Tuff

* Author for correspondence: rozsap@puma.unideb.hu

Table 1 Petrographic name, lithostratigraphic formation and locality of the samples

No.	Petrographic name	Lithostratigraphic formation	Locality
1	rhyodacite flood-tuff	Felnémet Rhyolite Tuff F.	Eger, Szépasszony Valley
2	rhyodacite tuff-tuffite	Kozárd Formation	Eger-Felnémet, Szarvaskői road
3	rhyodacite flood-tuff	Harsány Rhyolite Tuff F.	Eger-Felnémet, Bajusz Field
4	pumiceous breccia	Gyulakeszi Rhyolite Tuff F.	Eger, Ostorosi road
5	rhyodacite flood-tuff	Gyulakeszi Rhyolite Tuff F.	Eger-Tihamér, Alsó quarry
6	redeposited rhyodacite tuff	Harsány Rhyolite Tuff F.	Eger-Felnémet, Csurgó Valley
7	redeposited rhyodacite tuff	Felnémet Rhyolite Tuff F.	Eger, city wall
8	rhyodacite flood-tuff	Harsány Rhyolite Tuff F.	Eger, camping
9	rhyodacite tuff	Felnémet Rhyolite Tuff F.	Eger, Kőlyuktető
10	rhyodacite tuff	Harsány Rhyolite Tuff F.	Eger, Szala ditch

Formation (Badenian–Sarmatian), one sample was collected from tuffaceous bed of the Kozárd Formation (Sarmatian), and four ones come from the Harsány Rhyolite Tuff Formation (Badenian–Lower Pannonian) (Table 1). Description of the formations can be read in the explanatory book for the 1:100000 surface geological map series of Hungary [11], and several papers have given detailed petrographic characterisation of the tuffs in the area [12–14].

Sample preparation and density measurements were carried out in the Department of Mineralogy and Geology, University of Debrecen. Each sample was pulverized in agate mortar and dried in desiccator for two days. Density of the pulverized samples was measured by picnometer. Different types of bound waters were determined by using Mettler-Toledo TGA/SDTA 851^o thermo-microbalance equipment. 50–60 mg of the pulverized samples was analysed under static air atmosphere in the heating interval ranging from 25 to 1000^oC at a heating rate of 10^oC min⁻¹. For measurements aluminium-oxide crucibles of 150 μ L were used.

To identify mineralogical composition of the samples X-ray powder diffraction was carried out in the X-ray laboratory of University of Miskolc, Department of Mineralogy and Petrology. A Bruker D8 Advance type diffractometer was used, equipped with a ceramic X-ray tube with Cu anode and long fine focus. For the measurements fixed slit system and a dynamic scintillation detector was applied with secondary graphite monochromator. The X-ray beam was produced by 40 kV accelerating voltage and 40 mA tube current. Identification of the phases was implemented by Search/Match option of EVA 11, Release 2005 software. Semiquantitative analysis of the identified phases was performed by full pattern matching procedure of the Diffrac plus Basic Evaluation Package software (EVA 11, Release 2005) without standards. Global fitting of the measured scan with another one, simulated from the PDF patterns, was applied by using an empirical model for the peak shape. The method used

the I/I_{cor} coefficients from the PDF data file. It was assumed that the sum of all concentration was equal to 100%. Fitting of the scans were performed by pseudo-Voigt functions as a function of 2θ . For each PDF pattern, a scan was simulated, using the positions and peak heights from the patterns and the width and shape factors of the default model provided by the EVA software. A scaling factor and the width factors were then adjusted for each pattern, in order to minimize the discrepancy between the sum of the simulated and the measured scan. X-ray amorphous components of the samples were determined by limiting the backgrounds of the scans by Bézier curves [15].

The major components of the samples were analysed in the Laboratory of the Geological Institute of Hungary by using a Jobin Yvon ULTIMA 2C combined (simultaneous-sequential) ICP-OES instrument. First, 0.5 g of each rock samples was weighed into platinum crucibles, and then 1.16 g of LiBO₂ was added and mixed thoroughly. Crucibles were covered with platinum lids and were placed into electric furnace. Temperature was gradually increased up to 1060^oC. Reaching final temperature, samples were fused for 30 min. Crucibles were allowed to cool and then transferred into 100 mL glass beakers, covered with sufficient amount (about 50 mL) of deionised water and 10 mL of 1:1 HCl. The fusion melt was dissolved on a magnetic stirrer plate. After complete dissolution solution was transferred into volumetric flask and made up to 250 mL. (Total dissolved solid content is 2.0 g L⁻¹. Ten times dilution of this stock solution (0.2 g L⁻¹) was used for the major component determination. The ICP-OES instrument operating parameters are the next: RF power – 1000 W; reflected power – <10 W; plasma gas flow rate – 12 L min⁻¹; sheath gas flow rate – 0.2 L min⁻¹; nebuliser type – cross-flow; nebuliser flow rate – 0.4 L min⁻¹; nebuliser pressure – 2.7 bar; observation height – 15 mm (above load coil); integration time – 0.5 s (poly) to 5 s (mono). For purging the

monochromator for the determination of the UV lines nitrogen generator was applied. The $-H_2O$ and $+H_2O$ content were determined by gravimetric method, the FeO content was analysed by redox titration with $KMnO_4$ solution followed by decomposition with a mixture of H_2SO_4 and H_2F_2 in platinum crucible.

Results and discussion

Results of the X-ray powder diffraction analyses are summarised in Table 2. As it shows plagioclase of composition varying from albite to labradorite is the essential primary mineral constituent for most of the samples; its lowest quantity is 7% (sample 4), and the highest one is 56% (sample 8), but at least 18% for the

other samples. Quartz can be found in highest quantity in the samples 2 (33%) and 6 (24%) that exceed the amount of the plagioclase feldspar in these cases (19 and 18%, respectively). Moreover, 4% of biotite, and 2–3% of sanidine can be detected in samples 1 and 2, respectively. Amorphous material, which can be regarded as volcanic glass, represents significant constituent for each samples ranging from 21 (sample 8) to 60% (sample 1). Clay minerals (mostly illite, montmorillonite and vermiculite, rarely nontronite and sepiolite) are the most common secondary minerals. Beside clay minerals, small quantity of gypsum, erionite-like zeolite and alunogen can be also detected. On the basis of the proportion of the secondary minerals, sample 1 can be considered as relatively unaltered one, while sample 4

Table 2 Mineralogical composition of the studied samples.

Nr.	Primary minerals	Amorphous	Secondary minerals
1	37% (pl: 25%, qz: 8%, bi)	60%	3% (gy)
2	55% (qz: 33%, pl: 19%, sa)	34%	11% (al: 4%, il: 3%, ve, mm)
3	48% (pl: 38%, qz: 10%)	30%	22% (il: 9%, ve: 9%, mm)
4	10% (pl: 7%, qz: 3%)	42%	48% (mm: 32%, no: 7%, er: 4%, se: 3%, ve, gy)
5	50% (pl: 37%, qz: 13%)	38%	12% (il)
6	42% (qz: 24%, pl: 18%)	29%	29% (mm: 24%, il: 4%, ve)
7	55% (pl: 41%, qz: 14%)	30%	15% (il)
8	67% (pl: 56%, qz: 11%)	21%	12% (il: 11%, sm)
9	37% (pl: 30%, qz: 7%)	52%	11% (mm: 6%, ve)
10	47% (pl: 36%, qz: 11%)	39%	14% (il: 13%, sm)

Table 3 Major element composition, CIA values and density (ρ [g cm⁻³]) of the studied samples

	1	2	3	4	5	6	7	8	9	10
SiO ₂	68.3	64.1	66.2	55.9	69.3	69.6	69.1	70.2	67.1	65.8
TiO ₂	0.179	0.435	0.321	0.529	0.244	0.362	0.246	0.230	0.276	0.250
Al ₂ O ₃	13.1	13.8	14.7	15.6	13.2	12.5	14.4	14.0	13.9	13.8
Fe ₂ O ₃	1.51	3.95	2.27	3.93	1.42	3.12	1.39	0.91	1.73	2.17
FeO	0.09	0.25	0.63	0.35	0.78	0.28	0.77	0.64	0.78	0.21
MnO	0.041	0.054	0.048	0.074	0.055	0.031	0.034	0.027	0.042	0.041
CaO	2.60	1.92	2.94	2.83	3.10	1.85	2.56	2.54	1.99	2.77
MgO	0.500	0.543	0.818	1.10	0.705	0.451	0.536	0.493	0.367	0.719
Na ₂ O	2.16	1.28	1.91	1.17	2.36	1.68	2.48	2.45	2.17	2.52
K ₂ O	4.89	2.03	3.97	1.93	3.34	2.23	4.24	3.73	3.88	3.76
$-H_2O$	0.96	4.36	1.96	6.50	1.20	3.14	0.81	0.96	1.81	2.36
$+H_2O$	4.98	6.26	4.11	9.50	4.12	4.58	3.14	3.63	5.72	5.20
SO ₃	0.474	0.766	–	0.414	–	–	–	–	–	0.196
Σ	99.78	99.75	99.88	99.83	99.82	99.82	99.71	99.81	99.77	99.8
CIA	50.52	64.35	53.76	64.77	50.4	59.83	52.21	52.74	55.28	51.76
ρ	2.3217	2.2960	2.2641	2.1357	2.4054	2.3657	2.3862	2.3740	2.3089	2.3426

al – alunogen, bi – biotite, er – erionite-like zeolite, gy – gypsum, il – illite, mm – montmorillonite, no – nontronite, pl – plagioclase, qz – quartz, sa – sanidine, se – sepiolite, sm – smectite, ve – vermiculite

represents the most weathered type; the other samples are varying but moderately altered.

Major element composition and density of the studied samples is listed in Table 3. Silica content of the samples vary in wide interval, partly due to the varying degree of alteration, however, it reflects their rather rhyodacitic than rhyolitic character. Amounts of Fe_2O_3 , FeO and CaO are low, while alkali-oxides (particularly that of potassium-oxide) contents are high. Some tenth-percentages amount of sulphur in samples 1, 2 and 4 is in connection some gypsum ($\text{CaSO}_4 \cdot 2\text{H}_2\text{O}$) and alunogen ($\text{Al}_2[\text{SO}_4]_3 \cdot 18\text{H}_2\text{O}$) content detected by X-ray diffraction analyses. Based on major element composition, several indices of weathering degree have been proposed, however, the so called chemical index of alteration (CIA) [16] is the most widely used and the most accepted one [6, 17, 18]. This index can be calculated molar proportion of aluminium-, calcium- and alkali-oxides as it follows:

$$\text{CIA} = [\text{Al}_2\text{O}_3 / (\text{Al}_2\text{O}_3 + \text{CaO}^* + \text{Na}_2\text{O} + \text{K}_2\text{O})]$$

where CaO^* represents the CaO associated with the silicate fraction. Calculated CIA values for the studied samples are listed in Table 3. According to the CIA values, sample 4 is the most altered one, and samples 1 and 5 can be regarded to be relatively unaltered. Relationship between mineralogical composition and CIA index can be displayed on a secondary minerals vs. CIA diagram (Fig. 1). The figure indicates an obvious but moderate correlation between the secondary mineral content and CIA values of the samples. The extraordinary position of sample 2 is due to the some % presence of alunogen. Without this sample a strong correlation can be experienced (dotted trend line in Fig. 1).

Water content of the samples is characteristically high (particularly, the $+\text{H}_2\text{O}$ values) and extremely variable indicating the advance of the alteration processes. As Fig. 2 shows, there is moderate correlation of secondary mineral content to $+\text{H}_2\text{O}$, $-\text{H}_2\text{O}$ and total water content ($\text{H}_2\text{O}^{\text{total}}$). Comparing water content to CIA, it must be noted that $-\text{H}_2\text{O}$ data are in relatively close correlation to CIA values (Fig. 3). The measured density values are in negative connection with $\text{H}_2\text{O}^{\text{total}}$ (Fig. 4). On the basis of the linear trend of increasing density with decreasing total water content, an apparent density of 2.46 g cm^{-3} can be estimated for unaltered tuff, which is in quite good agreement with other calculation (2.44 g cm^{-3}) [2].

Amount of different types of bound water was measured by thermogravimetry. As Fig. 5 shows, although different water types form a continuous sequence [7], three thermal intervals and, consequently, three groups of bound water can be distinguished. Up to ca. $200\text{--}220^\circ\text{C}$ adsorption water, interlayer water and some part of crystal water is released. Between ca. $200\text{--}220$ and $500\text{--}550^\circ\text{C}$ first of all the water of the

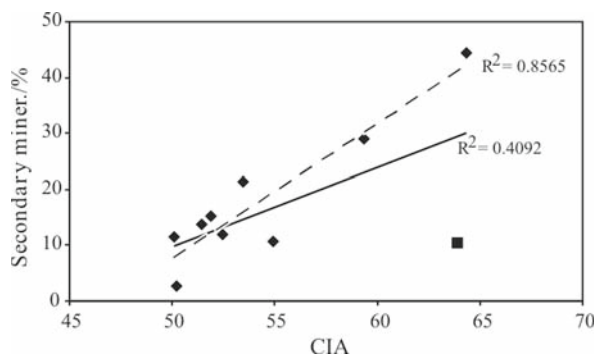


Fig. 1 Secondary minerals vs. CIA values for the studied samples (■ – sample 2)

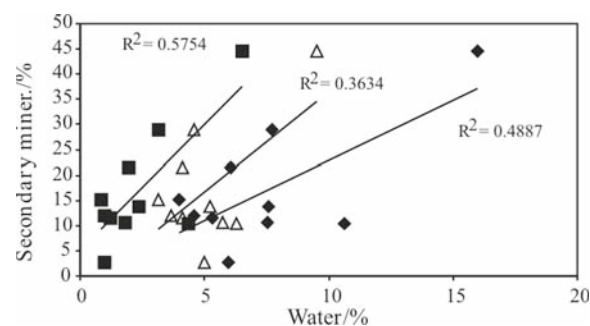


Fig. 2 Water content vs. secondary mineral content for the studied samples; ■ – $-\text{H}_2\text{O}$; △ – $+\text{H}_2\text{O}$; ◆ – $\text{H}_2\text{O}^{\text{total}}$

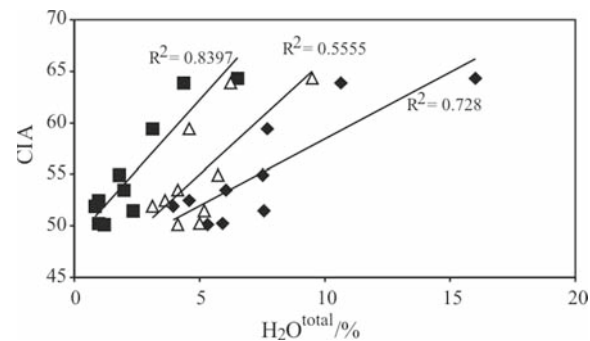


Fig. 3 Correlation between water content and CIA values of the studied samples; ■ – $-\text{H}_2\text{O}$; △ – $+\text{H}_2\text{O}$; ◆ – $\text{H}_2\text{O}^{\text{total}}$

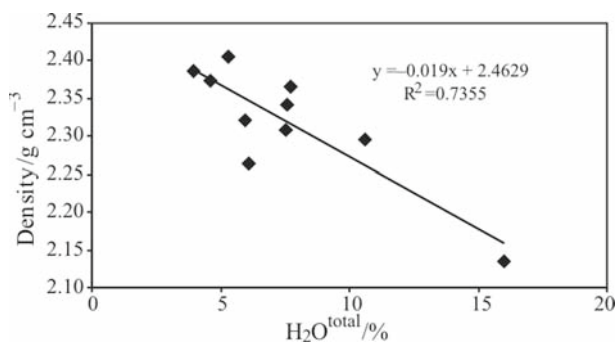


Fig. 4 Correlation between density and total water content ($\text{H}_2\text{O}^{\text{total}}$) of the studied samples

Table 4 TG parameters ($\Delta m\%$) of the studied samples

	1	2	3	4	5	6	7	8	9	10
H ₂ O(I)	1.12	5.23	2.25	6.80	1.79	3.69	0.95	1.24	2.18	2.29
H ₂ O(II)	3.30	1.12	2.10	4.20	2.37	1.31	2.12	2.33	3.04	2.66
H ₂ O(III)	0.53	2.88	1.40	3.27	1.11	2.16	0.87	0.66	2.00	2.00
H ₂ O(I+III)	1.65	8.11	3.65	10.07	2.90	5.85	1.82	1.90	4.18	4.29
H ₂ O ^{total}	4.95	9.23	5.75	14.27	5.27	7.16	3.94	4.23	7.22	6.95
SO ₃	0.87	1.04	–	0.84	–	–	–	–	–	–

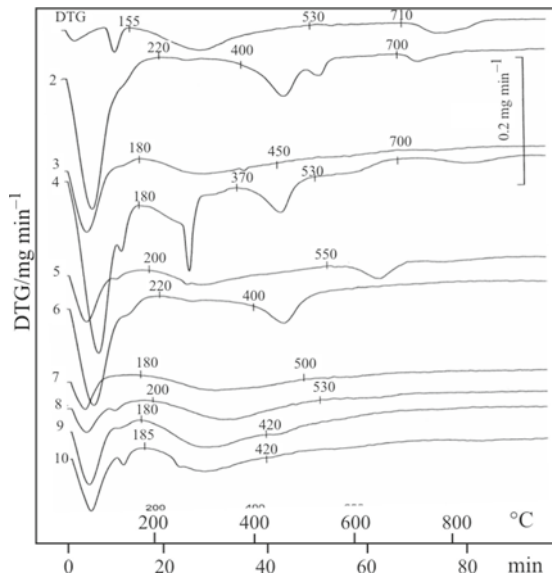


Fig. 5 DTG curves of the studied samples

amorphous rock glass is lost [7]. Above 500°C water is released mainly because of dehydroxylation of clay minerals produced by weathering. The above mentioned three groups of bound water are indicated as H₂O(I), H₂O(II) and H₂O(III), respectively; the measured H₂O(I), H₂O(II) and H₂O(III) values are listed in Table 4. Double-peak pattern of the H₂O(I) regime in the case of sample 1 indicates presence of gypsum as essential secondary mineral, while the considerable water loss of sample 2 in the same regime is in connection to alunogen. The mass loss detected above 700°C in the cases of samples 1 and 2 is due to mainly SO₃ release; therefore, it also indicates the presence of these sulphate minerals. In sample 4 small amount of SO₃ release also refer to gypsum, however, its double-peak in the H₂O(I) regime may be overlapped by absorbed water of much higher quantity coming from clay minerals. The relatively high iron content and the DTG curve suggest presence of Fe-bearing phase, however, it may be X-ray amorphous hydrous iron compound.

Quantity of H₂O(II) shows no correlation to either secondary mineral content or CIA, however, as it can be assumed on the basis of previous studies [7], it tends to increase with increasing amount of the amorphous material (Fig. 6). The extreme high H₂O(II) content in

sample 4 indicates presence of zeolite. Without this sample, there would be a definite negative correlation of H₂O(II) to both CIA and secondary mineral content (dotted trend line in Fig. 6).

H₂O(I), H₂O(III) and, consequently, H₂O(I+III) positively correlate to the amount of the secondary

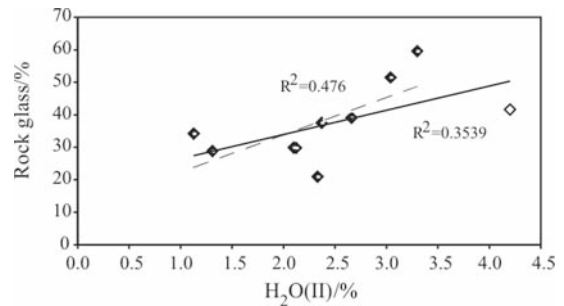


Fig. 6 H₂O(II) values vs. amorphous material content for the studied samples (\diamond – sample 4)

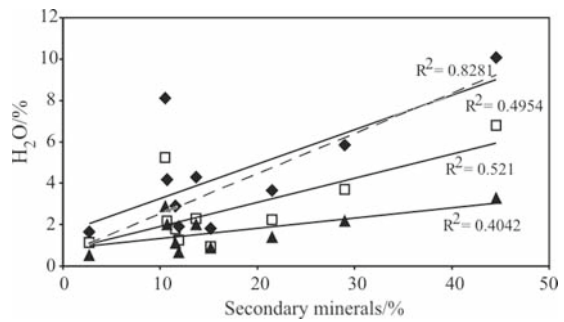


Fig. 7 Correlation of different types of bound water to the secondary mineral content; \blacktriangle – H₂O(III); \square – H₂O(I); \blacklozenge – H₂O(I+III)

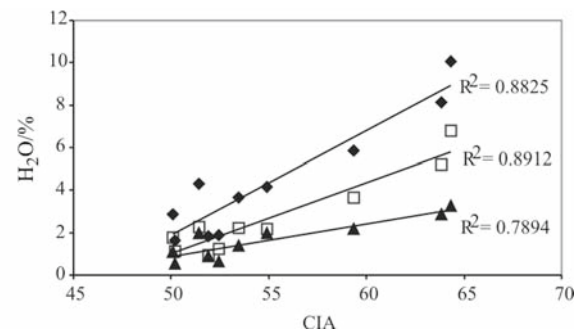


Fig. 8 Correlation of different types of bound water to CIA values; \blacktriangle – H₂O(III); \square – H₂O(I); \blacklozenge – H₂O(I+III)

minerals (Fig. 7). Similarly to the relationship between CIA and secondary minerals, the correlation is much closer if sample 2 was not taken into consideration (dotted trend line on Fig. 7). It is also noteworthy that correlations of H₂O(I) and H₂O(III) to secondary mineral content are almost the same than that of CIA to secondary minerals (Fig. 1). Consequently, there is a very close positive correlation of H₂O(I), H₂O(III) and H₂O(I+III) data to CIA values (Fig. 8).

Conclusions

Due to weathering water in the internal structure of minerals successively increases, i.e., increasing alteration involves increasing water content. Using thermogravimetry, distinction of different types of bound waters in minerals is possible. Comparing of mineralogical and major element composition and data of different types of bound water the following relationships were found:

- Amount of secondary minerals shows obvious but moderate positive correlation to CIA as well as H₂O(I), H₂O(III) and H₂O(I+III) values.
- Correlation of secondary mineral content and CIA is quite similar to that of secondary mineral content and H₂O(I), H₂O(III) and H₂O(I+III). H₂O(II) shows no correlation to both secondary mineral content and CIA, however, it is in positive correlation to amount of amorphous material.
- CIA is in close positive correlation to H₂O(I), H₂O(III) and H₂O(I+III) values. These correlations are, in general, remarkably closer than that of CIA to total water content (H₂O^{total}) or even to -H₂O.

Considering the above mentioned relationships, it can be concluded that validity of some TG H₂O parameters, such as H₂O(I), H₂O(III) and H₂O(I+III) for indicating alteration of rocks is very similar to that of CIA. It would be desirable to determine more precise correlation between TG H₂O parameters and CIA, however it requires further studies on numerous samples. Recently, some authors emphasised that geochemical signatures of weathering should be used to establish a framework for further interpretation and prediction rather than quick classifications using different indices [6]. By using thermogravimetric methods, not simply the different types of bound water can be determined, but essential petrographical and mineralogical conclusions can be drawn concerning the weathering process, too [7]. Consequently, thermogravimetry, and other thermal analytical methods, may serve not simply as useful tool for estimation and characterisation of weathering degree of rocks, but might be considered as an essential part of this framework.

Acknowledgements

The authors dedicate this paper to the memory of the late Gyula Szöör, emeritus professor of the Department of Mineralogy and Geology, University of Debrecen, who initiated and inspired this research. The authors thank Viktor Má dai (University of Miskolc) for evaluating of amorphous content, and Judit Szabolcsi for her help in collecting the samples. This work has been supported by the Hungarian National Science Research Foundation (OTKA) under Res. Contracts No. T046579.

References

- 1 H. C. Helgeson, R. M. Garrels and F. T. Mackenzie, *Geochim. Cosmochim. Acta*, 33 (1969) 455.
- 2 B. Kleb and B. Vásárhelyi, *Acta Geol. Hung.*, 46 (2003) 301.
- 3 Gy. Szöör and E. Pittlik, Á. Kézdi and I. Lazányi Eds, *Proceedings of the Fifth Budapest Conference on Soil Mechanics and Foundation Engineering*, Akadémiai Kiadó, Budapest 1976, pp. 201–210.
- 4 Gy. Szöör, *Bull. Hung. Geol. Soc.*, 108 (1978) 577. (in Hungarian).
- 5 T. Esaki and K. Jiang, *Eng. Geol.*, 55 (1999) 121.
- 6 N. S. Duzgoren-Aydin, A. Aydin and J. Malpas, *Eng. Geol.*, 63 (2002) 99.
- 7 M. Földvári, F. Paulik and J. Paulik, *J. Thermal Anal.*, 33 (1998) 121.
- 8 M. Földvári and P. Kovács-Pálffy, *Acta Geol. Hung.*, 45 (2002) 247.
- 9 K. H. Ip, B. H. Stuart, P. S. Thomas and A. S. Ray, *J. Therm. Anal. Cal.*, 92 (2008) 97.
- 10 J.M.P. Garcia, H.F. Mothé Filho and L.V. Zuquete, *J. Therm. Anal. Cal.*, 93 (2008) 253.
- 11 L. Gyalog, Ed., *Explanatory to covered geological map of Hungary 1:100000*, Geological Institute of Hungary, Budapest 2005 p. 189 (in Hungarian).
- 12 A. Szakács, I. Seghedi, T. Zelenka, E. Márton, Z. Pécskay and T. Póka, *Acta Geol. Hung.*, 41 (1998) 401.
- 13 T. Póka, T. Zelenka, A. Szakács, I. Seghedi, G. Nagy and A. Simonovits, *Acta Geol. Hung.*, 41 (1998) 437.
- 14 E. Márton and Z. Pécskay, *Acta Geol. Hung.*, 41 (1998) 467.
- 15 C. R. Hubbard, E. H. Evans and D. K. Suith, *J. Appl. Cryst.*, 9 (1976) 169.
- 16 H. W. Nesbitt and G. M. Young, *Geochim. Cosmochim. Acta*, 48 (1984) 1523.
- 17 H. Rollinson, *Using geochemical data*, Longman, Harlow 1998, p. 352.
- 18 A. Varga, Gy. Szakmány, B. Raucsik, Zs. Hartyáni, V. Szilágyi and T. Horváth, *Hung. J. Chem.*, 108 (2002) 387 (in Hungarian).

Received: July 6, 2008

Accepted: October 6, 2008

Online First: April 13, 2009

DOI: 10.1007/s10973-008-9386-3